Multi-Target Tracking on Riemannian Manifolds via Probabilistic Data Association

Borna Bićanić, *Student Member, IEEE*, Ivan Marković, *Member, IEEE*, Ivan Petrović, *Member, IEEE*

***Abstract*—Riemannian manifolds are attracting much interest in various technical disciplines, since generated data can often be naturally represented as points on a Riemannian manifold. Due to the non-Euclidean geometry of such manifolds, usual Euclidean methods yield inferior results, thus motivating development of tools adapted or specially tailored to the true underlying geometry. In this letter we propose a method for tracking multiple targets residing on smooth manifolds via probabilistic data association. By using tools of differential geometry, such as exponential and logarithmic mapping along with the parallel transport, we extend the Euclidean multi-target tracking techniques based on probabilistic data association to systems constrained to a Riemannian manifold. The performance of the proposed method was extensively tested in experiments simulating multi-target tracking on unit hyperspheres, where we compared our approach to the von Mises-Fisher and the Kalman filters in the embedding space that projects the estimated state back to the manifold. Obtained results show that the proposed method outperforms the competitive trackers in the optimal sub-pattern assignment metric for all the tested hypersphere dimensions. Although our use case geometry is that of a unit hypersphere, our approach is by no means limited to it and can be applied to any Riemannian manifold with closed-form expressions for exponential/logarithmic maps and parallel transport along the geodesic curve. The paper code is publicly available[1].**

***Index Terms*—Riemannian geometry, multi-target tracking, probabilistic data association**

I. Introduction

MANY challenging problems arise in multi-target tracking (MTT) compared to classical estimation such as missing detections, false alarm, uncertainty in measurement origin and many others [1]. Most of the state-of-the-art MTT algorithms can be divided in three groups with respect to how they treat the unknown measurement origin (data association): (i) probabilistic data association (PDA), (ii) multiple hypothesis tracking (MHT) and (iii) random finite sets (RFS) tracking. PDA and its variants [2]–[4] calculate posterior association probabilities between tracks and received detections and then update each target with the weighted sum of detections. MHT methods [5], [6] handle the detection origin uncertainty by creating a tree of possible association hypotheses. The tree is created recursively while the unlikely hypotheses are discarded to reduce the computational load. RFS tracking methods [7]–[10] are paradigm that does not solve the data assignment problem directly but rather formulate the tracking as filtering on random finite sets [11]. Regardless of the MTT approach, the underlying geometry of the tracked targets state does not have to necessarily reside on the Euclidean space. For example, some sensor examples report angle- or direction-only measurements [12], [13], moving objects might evolve on constrained spaces [14], [15], and in visual tracking the appearance of an object is captured by deep features that can be described with Riemannian geometry [16], [17].

Non-Euclidean spaces have recently been addressed in many robotic and computer vision applications [18], [19]. Rigid body pose is naturally an element of the Lie group, hence state-of-the-art simultaneous localisation and mapping (SLAM) and pose estimation algorithms use this fact to form the underlying state space for estimation [20]–[24]. Other examples of using non-Euclidean geometry can be found in state estimation and tracking on directional only data, which can be accomplished by utilizing directional distributions, such as the von Mises-Fisher (vMF) or the Bingham distribution [25]–[29]. In visual tracking, object appearance is very useful in the detection-to-target association procedure which can be represented using hand-crafted features [30]–[32] or deep neural network features [17], [33]–[36]. Both directional only data and covariance features lie on smooth metric spaces called Riemannian manifolds (RMs) [19]. Visual tracking applications can use the geometry of those spaces to find the optimal assignment between detected and tracked objects [37], but they often ignore the dynamics of objects and the uncertainty of deep features. Nonetheless, filtering methods involving RM valued systems have been introduced in [15], [16], [38]–[43].

In this letter, we propose a method for tracking multiple targets on smooth manifolds via probabilistic data association. Our main contribution lies in extending the principle of probabilistic data association to multitarget tracking on Riemannian manifolds. To achieve this we leverage the RM unscented Kalman filter [40] and alter the update step to enable a probabilistically weighted update with a varying number of measurements. To ensure semi-positive definiteness of the posterior covariance, we apply the Joseph form of the Kalman filter update [44]. Using the novel equations, we implement the RM joint integrated probabilistic data association (JIPDA) tracker. We conducted extensive experiments simulating MTT on unit hyperspheres ranging from the circle to 15-dimensional unit sphere. We compared our approach to the vMF JIPDA [29] and the Kalman filter in the embedding space that projects the estimated state back to the manifold. As performance metric we use the optimal sub-pattern assignment metric (OSPA). Although our use case is that of a unit hypersphere, our approach is by no means limited to it and can be applied to any RM with closed-form expressions for exponential/logarithmic maps and parallel transport along the geodesic curve.

B. Bićanić, I. Marković and I. Petrović are with the University of Zagreb, Faculty of Electrical Engineering and Computing, Unska 3, 10000 Zagreb, Croatia. E-mail: {name.surname@fer.hr}

This research has been supported by the European Regional Development Fund under the grant KK.01.1.1.01.0009 (DATACROSS).

[1]MATLAB code is available at https://bitbucket.org/unizg-fer-lamor/m3t.

Fig. 1: Exp and Log maps of a Riemannian manifold $\mathcal{M}$ (left) and parallel transport of tangent vectors along γ (right).

II. Riemannian Geometry

A Riemannian manifold $\mathcal{M}$ is a differentiable d-dimensional topological space that is equipped with the positive definite metric tensor g – the Riemann metric tensor that depends smoothly on the point $p \in \mathcal{M}$. At each point p, an RM can be locally approximated by the tangent space $T_p\mathcal{M}$ equipped with the scalar product $\langle u, v\rangle_p = u^T g(p)\, v$, that allows us to measure curves and angles between curves on a manifold [45]. The distance between two points $x, y \in \mathcal{M}$ denoted by $d(x, y)$ induced by the metric tensor is the length of the shortest curve between x and y. A smooth curve $\gamma(t)$ that minimizes this length is called a geodesic and it satisfies $\nabla_{\dot\gamma(t)}\dot\gamma(t) = 0$, where $\nabla_u v$ represents the covariant derivative [45]. Exponential map $\mathrm{Exp}_x : T_x\mathcal{M} \to \mathcal{M}$ brings the tangent vector $u \in T_x\mathcal{M}$ to the point $y \in \mathcal{M}$ such that the x and y are connected by the geodesic in direction u of the length $\|u\|_x$. The inverse mapping, if it exists, is called logarithmic mapping and is denoted as $\mathrm{Log}_x : \mathcal{M} \to T_x\mathcal{M}$. To compare tangent vectors at different points of $\mathcal{M}$, they must be parallelly transported to the same tangent space. However, this operation depends on the path through which the vector is transported. Parallel transport of a tangent vector u along the curve $\gamma(t)$ is given by the expression $\nabla_{\dot\gamma(t)}u(t) = 0$. Parallel transport of a vector u along a shortest geodesic between points $x, y \in \mathcal{M}$ is denoted by $\mathrm{P}_{x\to y}(u)$. These notions are illustrated in Fig. 1.

A. Statistics on Riemannian Manifolds

The mean of N points, $\{x_1, ..., x_n\} \in \mathcal{M}$, can be calculated as the Kärcher mean by minimizing the quadratic error [19]

$$\mu = \arg\min_x \frac{1}{N}\sum_{i=1}^{N} d^2(x, x_i). \tag{1}$$

When points are close enough, a unique global solution called the Fréchet mean can be computed using the Gauss-Newton optimisation. The covariance matrix of points $\{x_1, ..., x_n\}$ in the tangent space $T_\mu\mathcal{M}$ is $\Sigma = \frac{1}{N}\sum_{i=1}^{N}\mathrm{Log}_\mu(x_i)\mathrm{Log}_\mu(x_i)^T$.

To generalise a Gaussian distribution to RMs, it is defined in the tangent space at its mean value [19]

$$\mathcal{N}_\mathcal{M}(x \mid \mu, \Sigma) = \frac{1}{\sqrt{\det(2\pi\Sigma)}}\exp\left(-\frac{1}{2}d_M^2(\mu, x)\right), \tag{2}$$

where $d_M(\mu, x) = \sqrt{\mathrm{Log}_\mu(x)^T\,\Sigma^{-1}\,\mathrm{Log}_\mu(x)}$ is the generalised Mahalanobis distance.

B. Sphere as a manifold

The proposed approach can be applied to any RM but in this letter, as a case study, we take the n-dimensional sphere. An n-dimensional sphere of radius ρ, $\mathcal{S}^n_\rho = \{x \in \mathbb{R}^{n+1} : x^T x = \rho^2\}$, is an RM with the metric tensor induced by the ambient Euclidean space $\mathbb{R}^{n+1}$ [46]. Thus, the scalar product of tangent vectors u and v at point $x \in \mathcal{S}^n_\rho$ is $\langle u, v\rangle_x = u^T v$, i.e. the metric tensor, is the identity matrix. The distance between $x, y \in \mathcal{S}^n_\rho$ can be computed as [46]

$$d(x, y) = \rho \arccos\frac{x^T y}{\rho^2} \tag{3}$$

defining great circles as the geodesic lines. The exponential map of the tangent vector u at point x is defined as [19]

$$\mathrm{Exp}_x(u) = x\cos\frac{\|u\|}{\rho} + \frac{u}{\|u\|}\rho\sin\frac{\|u\|}{\rho}, \tag{4}$$

while the logarithmic map amount to the following expression

$$\mathrm{Log}_x(y) = d(x, y)\frac{\rho^2\, y - x^T y\, x}{\|\rho^2\, y - x^T y\, x\|}. \tag{5}$$

Parallel transport of a tangent vector u from point x to point y along a geodesic is finally given by [19]

$$\mathrm{P}_{x\to y}(u) = u - \frac{\mathrm{Log}_x(y)^T u}{d^2(x, y)}\left[\mathrm{Log}_x(y) + \mathrm{Log}_y(x)\right]. \tag{6}$$

In the implementation, we have used two local coordinate charts (stereographic projections) to cover the whole sphere – details are relegated to the supplementary materials.

III. PDA on Riemannian Manifolds

To solve the problem of unknown measurement to track correspondence in MTT, it is often advantageous to use probabilistic data association rather than making hard decisions on measurements' origin – an example is the JIPDA filter [4]. To avoid considering all possible joint association events between targets and detections a measurement gating procedure is often used to reduce computational complexity.

Let $X^k = \{x_{1,k}, ..., x_{n_k,k}\}$, where n_k is the number of targets at time k, denote the set of all targets at time k and similarly let $Z^k = \{z_{1,k}, ..., z_{m_k,k}\}$ be the set of all detections at time k where m_k is the number of detections. In the letter we denote the predicted and updated state and covariance with the $^-$ and $^+$ superscript, respectively. Since we are dealing with the tracking on RMss, which are, in general, nonlinear spaces, vector space Kalman filter cannot be applied. An example of 5 targets evolving on $\mathcal{S}^2$ can be seen in Fig. 2. Nonetheless, generalisations of the Kalman filter to

Fig. 2: MTT on the sphere. Ground truth trajectories (left) and the Riemannian manifold JIPDA tracking result (right).

RM have been introduced [40], [41]. In this letter, we utilize the unscented Kalman filter (UKF) variant [40]; however, the following holds as well for the extended version. To derive the JIPDA on RMs (RM-JIPDA), several new building block are needed, which we present in the sequel.

A. RM-JIPDA prediction

Given the state $\hat{x}^+_{j,k-1}$ and covariance $P^+_{j,k-1}$ of j-th target at time $k-1$, sigma vectors on the tangent space $T_{\hat{x}^+_{j,k-1}}\mathcal{M}$ are obtained by the following formulae

$$v^i_{j,k-1} = \sqrt{d+\lambda} \cdot L_{i,j}, \qquad i = 1, ..., d$$
$$v^{i+d}_{j,k-1} = -\sqrt{d+\lambda} \cdot L_{i,j}, \qquad i = 1, ..., d$$

where $L_{i,j}$ is the i-th column of the Cholesky factor of $P^+_{j,k-1}$. Sigma points are then obtained by projecting sigma vectors to $\mathcal{M}$ using the exponential map [40]

$$\sigma^0_{j,k-1} = \hat{x}^+_{j,k-1},$$
$$\sigma^i_{j,k-1} = \mathrm{Exp}_{\hat{x}^+_{j,k-1}}(v^i_{j,k-1}), \qquad i = 1, ..., 2d$$

Sigma points are then mapped by the nonlinear system tranistion model $f : \mathcal{M} \to \mathcal{M}$, $\sigma^i_{j,k} = f(\sigma^i_{j,k-1})$ and the predicted state is obtained by calculating (1) of weighted sigma points. Predicted covariance of the j-th target is then computed as

$$P^-_{j,k} = \sum_{i=0}^{2d} w_i \, v^i_{j,k} \, {v^i_{j,k}}^T + Q, \tag{7}$$

where Q is the covariance matrix of the process noise and w_i are weights of sigma points where $v^i_{j,k} = \mathrm{Log}_{\hat{x}^-_{j,k}}(\sigma^i_{j,k})$.

B. RM-JIPDA correction

Let $h : \mathcal{M} \to \mathcal{N}$ be the observation model, where $\mathcal{N}$ is the observation space. First we calculate the new set $\tilde{\sigma}^i_{j,k}$ given $\hat{x}^-_{j,k}$ and $P^-_{j,k}$ which are then mapped to the $\mathcal{N}$ as $\bar{\sigma}^i_{j,k} = h(\tilde{\sigma}^i_{j,k})$ and the predicted measurement $\hat{z}^-_{j,k}$ is the Kärcher mean of sigma points $\bar{\sigma}^i_{j,k}$.The innovation covariance matrix and the cross-covariance are [40]

$$S_{j,k} = \sum_{i=0}^{2d} w_i \, s^i_{j,k} \, {s^i_{j,k}}^T + R, \tag{8}$$

$$C_{j,k} = \sum_{i=0}^{2d} w_i \, v^i_{j,k} \, {s^i_{j,k}}^T, \tag{9}$$

where R is the covariance matrix of the measurement noise, $s^i_{j,k} = \mathrm{Log}_{\hat{z}_{j,k}}(\bar{\sigma}^i_{j,k})$ and $v^i_{j,k} = \mathrm{Log}_{\hat{x}^-_{j,k}}(\tilde{\sigma}^i_{j,k})$.

To reduce the complexity of the data association step, measurements are gated using the generalized χ^2 test in the tangent space of the prediction $T_{\hat{z}^-_{j,k}}\mathcal{N}$

$$\mathrm{Log}_{\hat{z}^-_{j,k}}(z_{i,k})^T \, S^{-1}_{j,k} \, \mathrm{Log}_{\hat{z}^-_{j,k}}(z_{i,k}) \le \chi^2_n(p_g), \tag{10}$$

where χ^2_n is the quantile function of n-dimensional χ^2 distribution, and the p_g is the gating probability. Given that the detection $z_{i,k}$ is validated, the likelihood of $z_{i,k}$ given the predicted detection $\hat{z}_{j,k}$ is $g_{i,j} = p_g^{-1}\mathcal{N}_{\mathcal{M}}(z_{i,k} \mid \hat{z}_{j,k}, S_{j,k})$, where p_g is gating probability.

Update equations of a Riemannian UKF [40] take only one measurement, however, in JIPDA there can be any number of measurements assigned to a single target. To extend those equations for the soft assignment we first define the innovation of i-th measurement to j-th target as $\nu_{i,j,k} = \mathrm{Log}_{\hat{z}_{j,k}}(z_{i,k})$. Total weighted innovation of all measurements for j-th target, given posterior association probabilities $\beta_{i,j,k}$ [17], [47], is

$$\nu_{j,k} = \sum_{i=1}^{m_k} \beta_{i,j,k} \, \nu_{i,j,k}. \tag{11}$$

Target j is then updated by following equation [40]

$$\hat{x}^+_{j,k} = \mathrm{Exp}_{\hat{x}^-_{j,k}}(K_{j,k} \, \nu_{j,k}), \tag{12}$$

where $K_{j,k} = C_{j,k} \, S^{-1}_{j,k}$ is the Kalman gain for the j-th target.

Next, we extend the covariance update equation of the Riemannian UKF [40] $P^+_{j,k} = P^-_{j,k} - K_{j,k} \, S_{j,k} \, K^T_{j,k}$. First, we apply the Joseph form of UKF update [44] to ensure that the posterior covariance is positive semi-definite matrix

$$P^+_{j,k} = A_{j,k} \, P^-_{j,k} \, A^T_{j,k} + K_{j,k} \, R \, K^T_{j,k}, \tag{13}$$

where $A_{j,k}$ stands for $I - K_{j,k} \, C^T_{j,k} {P^-_{j,k}}^{-1}$, and R is the covariance matrix of the measurement noise defined at $T_{\hat{z}_{j,k}}\mathcal{N}$. Equation (13) is exact when there is exactly one measurement, however, when there are multiple measurements, then the posterior covariance depends also on the number of measurements and their spread around the $\hat{z}_j$ [2]. This dependency can be expressed using the matrix $T_j = \sum_{i=1}^{m_k} \beta_{i,j} \, \nu_{i,j} \, \nu^T_{i,j} - \nu_j \, \nu^T_j$. Hence, final update equation is obtained by adding the term $K_{j,k} \, T_j \, K^T_{j,k}$ to (13)

$$P^+_{j,k} = A_{j,k} \, P^-_{j,k} \, A^T_{j,k} + K_{j,k} \, R \, K^T_{j,k} + K_{j,k} \, T_j \, K^T_{j,k}. \tag{14}$$

TABLE I: Average OSPA error for 100 Monte Carlo runs for different dimensions of the unit hypersphere state space.

	$\mathcal{S}^1$	$\mathcal{S}^2$	$\mathcal{S}^3$	$\mathcal{S}^4$	$\mathcal{S}^5$	$\mathcal{S}^{10}$	$\mathcal{S}^{15}$
RM-JIPDA	**0.3494**	**0.1182**	**0.0547**	**0.0371**	**0.0343**	**0.0277**	**0.0312**
vMF-JIPDA	0.3730	0.1544	0.0629	0.0429	0.0411	0.0395	0.0454
Proj-KF-JIPDA	0.4994	0.4683	0.3884	0.2982	0.2454	0.0929	0.9997

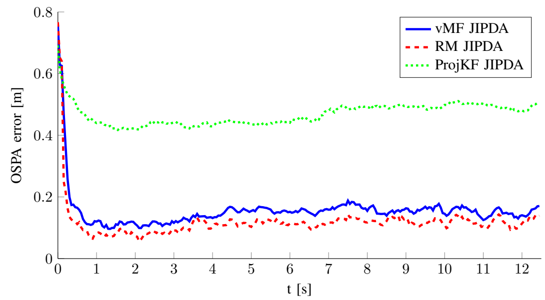

Fig. 3: Average OSPA error through time for the $\mathcal{S}^2$ case

Finally, all of the previous calculations are conducted in the tangent space of $\hat{x}^-_{j,k}$, and therefore, $P^+_{j,k}$ must be parallelly transported to the updated state $\hat{x}^+_{j,k}$ [40].

IV. Results

We evaluated our method in simulations and compared it to the JIPDA trackers that use the von Mises-Fisher (vMF) filter [29] and the Kalman filter whose state was projected back to the manifold after each update step (ProjKF). We conducted 100 Monte Carlo runs of a scenario where 5 objects evolved on a unit hypersphere of dimensions ranging from $\mathcal{S}^1$ to $\mathcal{S}^{15}$. An example of such a scenario for $\mathcal{S}^2$ is shown in Fig. 2. The simulation settings were as follows. Sampling time was $\Delta T = 0.05\,\mathrm{s}$ with single simulation duration of 250 steps. Ground truth trajectories were generated using discrete constant velocity model generalized to the RMs

$$x_k = \mathrm{Exp}_{x_{k-1}}(\Delta T \cdot v_{k-1}), \quad (15)$$

$$v_k = \mathrm{P}_{x_{k-1}\to x_k}\left(v_{k-1} + \Delta T \cdot w_k\right), \quad (16)$$

with Gaussian noise acceleration $w \sim \mathcal{N}\left(\cdot \mid 0, 0.9^2\, I_2\right)$. Starting positions and velocities of objects were chosen randomly. Detections were generated by adding measurement noise in the tangent space $v \sim \mathcal{N}(\cdot \mid 0, 0.002\, I_2)$ with the detection probability $p_d = 0.98$ and clutter rate of 0.5 false detections per step. Our JIPDA parameters were as follows: target survival probability $p_s = 0.99$, $p_d = 0.98$, gating probability $p_g = 0.95$, and false alarm rate $\lambda = 0.5$. New targets were given initial existence probability of $w_e = 0.65$, confirmed when $w_e \geq 0.85$, and terminated when $w_e \leq 0.003$.

Parameters of the vMF filter were: diffusion concentration $\kappa_d = 20$, observation concentration $\kappa_o = 8000$ and initial state concentration $\kappa_0 = 100$. Process noise covariance of the ProjKF was $Q = 0.2^2\, I_3$ with the measurement noise covariance $R = 0.002^2\, I_3$. Target motion and observation models were $F = H = I_3$ and the initial covariance was $P_0 = 0.004^2\, I_3$. Identity models $f(x) = x$ and $h(x) = x$ were also used in the UKF for RMs, where the process noise was random Gaussian variable in the tangent space of the state with $Q = 0.2^2\, I_2$ and $R = 0.002^2\, I_2$. Initial covariance of the targets' states was set to $P_0 = 0.004^2\, I_2$.

To measure the performance we used the OSPA metric [48] which penalizes both location and cardinality errors. We set cut-off distance of OSPA metric to $c = 1$ and the order $p = 2$. In Fig. 2 we can see an instance of the RM-JIPDA results for $\mathcal{S}^2$ together with the ground truth trajectories. There were no identity switches, but we can notice some spikes caused by spurious measurements and the drift of yellow and purple targets when they pass by each other. In Fig. 3 we show the average OSPA error through time for this experiment. As we can see, our method outperformed the vMF-JIPDA by $23.45\,\%$ while the ProjKF approach was barely applicable. The poor results of the the ProjKF approach are due to the error introduced by correcting the state in ambient Euclidean space and then projecting it back to the manifold – this error also inflates the covariance resulting in a higher number of identity switches and lost tracks. The results for other dimensions are shown in Table I from which we can see that the proposed method again outperformed both the vMF-JIPDA and ProjKF-JIPDA trackers. Furthermore, we have also conducted an experiment where measurements are generated on Euclidean space $\mathbb{R}^3$ as an example where hidden state and measurement do not lie on the same space. In that case the RM-JIPDA and vMF-JIPDA scored 0.1447 and 0.1464, respectively, and both outperformed Proj-KF by a large margin. One of the advantages of proposed method compared to vMF JIPDA is that it can better capture the uncertainty of targets, that is, the state of vMF can only be distributed isotropically around the mean. Also, there are many numerical challenges concerning vMF JIPDA, especially in higher dimensional systems [29].

V. Conclusion

In this letter we have proposed an MTT algorithm for targets that are constrained to curved subspaces of the Euclidean space called Riemannian manifolds. We extended the RM-UKF [40] in order to implement the probabilistic data association in a soft association approach to MTT required by the JIPDA filter. To validate the performance of our method, we conducted extensive experiments simulating MTT on a range of unit hyperspheres and compared our approach to the vMF- and ProjKF-JIPDA. We calculated the OSPA metric from 100 Monte Carlo simulation, and the results showed that the proposed method outperformed the competitive filters across all the hypersphere dimensions.

References

[1] B.-n. Vo, M. Mallick, Y. Bar-shalom, S. Coraluppi, R. Osborne, R. Mahler, and B.-t. Vo, "Multitarget Tracking," in *Wiley Encyclopedia of Electrical and Electronics Engineering*. Hoboken, NJ, USA: John Wiley & Sons, Inc., sep 2015, pp. 1–15.

[2] Y. Bar-Shalom and E. Tse, "Tracking in a cluttered environment with probabilistic data association," *Automatica*, vol. 11, pp. 451–460, 1975.

[3] T. Fortmann, Y. Bar-Shalom, and M. Scheffe, "Sonar tracking of multiple targets using joint probabilistic data association," *IEEE Journal of Oceanic Engineering*, vol. 8, no. 3, pp. 173–184, jul 1983.

[4] D. Mušicki and R. Evans, "Joint Integrated Probabilistic Data Association - JIPDA," in *Proceedings of the Fifth International Conference on Information Fusion. FUSION 2002.*, 2002.

[5] D. Reid, "An algorithm for tracking multiple targets," *IEEE Transactions on Automatic Control*, vol. 24, no. 6, pp. 843–854, 1979.

[6] C.-Y. Chong, S. Mori, and D. B. Reid, "Forty Years of Multiple Hypothesis Tracking - A Review of Key Developments," in *2018 21st International Conference on Information Fusion (FUSION)*. IEEE, jul 2018, pp. 452–459.

[7] B.-N. Vo and W.-K. Ma, "The Gaussian Mixture Probability Hypothesis Density Filter," *IEEE Transactions on Signal Processing*, vol. 54, no. 11, pp. 4091–4104, nov 2006.

[8] B.-T. Vo, B.-n. Vo, and A. Cantoni, "Analytic Implementations of the Cardinalized Probability Hypothesis Density Filter," *IEEE Transactions on Signal Processing*, vol. 55, no. 7, pp. 3553–3567, jul 2007.

[9] B.-T. Vo, B.-N. Vo, and A. Cantoni, "On multi-Bernoulli approximations to the Bayes multi-target filter," *Fusion2007*, 2007.

[10] S. Reuter, B. T. Vo, B. N. Vo, and K. Dietmayer, "The labeled multi-Bernoulli filter," *IEEE Transactions on Signal Processing*, vol. 62, no. 12, pp. 3246–3260, 2014.

[11] R. P. Mahler, *Statistical Multisource-Multitarget Information Fusion*. Boston: Artech House, INC., 2007.

[12] I. Markovic, A. Portello, P. Danes, I. Petrovic, S. Argentieri, I. Marković, A. Portello, P. Danès, and I. Petrović, "Active speaker localization with circular likelihoods and bootstrap filtering," in *IEEE/RSJ International Conference on Intelligent Robots and Systems (IROS)*, 2013, pp. 2914–2920.

[13] I. Marković, "Moving objects detection and tracking by omnidirectional sensors of a mobile robot," Ph.D. dissertation, University of Zagreb, Faculty of Electrical Engineering and Computing, 2014.

[14] S. Bhattacharjee, J. T. Kent, I. Hussein, and M. K. Jah, "Bayesian filtering using directional statistics for space debris tracking problem," in *IAA Symposium on Space Debris*, 2017.

[15] B. Starbuck, A. Fornasier, and S. Weiss, "Consistent State Estimation on Manifolds for Autonomous Metal Structure Inspection," in *International Conference on Robotics and Automation*, 2021.

[16] A. Tyagi and J. W. Davis, "A recursive filter for linear systems on Riemannian manifolds," in *2008 IEEE Conference on Computer Vision and Pattern Recognition*. IEEE, jun 2008, pp. 1–8.

[17] B. Bicanic, M. Orsic, I. Markovic, S. Segvic, and I. Petrovic, "Pedestrian Tracking by Probabilistic Data Association and Correspondence Embeddings," in *FUSION 2019 - 22nd International Conference on Information Fusion*, jul 2019.

[18] T. D. Barfoot, *State Estimation for Robotics*. Cambridge: Cambridge University Press, 2017.

[19] S. Calinon, "Gaussians on riemannian manifolds: Applications for robot learning and adaptive control," *IEEE Robotics and Automation Magazine*, vol. 27, no. 2, pp. 33–45, sep 2020.

[20] G. Bourmaud, R. Megret, A. Giremus, and Y. Berthoumieu, "Discrete Extended Kalman Filter on Lie groups," in *European Signal Processing Conference*, 2013.

[21] G. Bourmaud, R. Mégret, M. Arnaudon, and A. Giremus, "Continuous-Discrete Extended Kalman Filter on Matrix Lie Groups Using Concentrated Gaussian Distributions," *Journal of Mathematical Imaging and Vision*, vol. 51, no. 1, pp. 209–228, jan 2015.

[22] V. Joukov, I. Petrović, and J. Ćesić, "Full Body Human Motion Estimation on Lie Groups Using 3D Marker Position Measurements," *2016 IEEE-RAS International Conference on Humanoid Robots (Humanoids 2016)*, 2016.

[23] J. Cesic, I. Markovic, and I. Petrovic, "Moving object tracking employing rigid body motion on matrix Lie groups," in *FUSION 2016 - 19th International Conference on Information Fusion, Proceedings*, no. i, 2016, pp. 2109–2115.

[24] ——, "Mixture Reduction on Matrix Lie Groups," *IEEE Signal Processing Letters*, vol. 24, no. 11, pp. 1719–1723, nov 2017.

[25] K. V. Mardia and P. E. Jupp, *Directional Statistics*, ser. Wiley Series in Probability and Statistics, K. V. Mardia and P. E. Jupp, Eds. Hoboken, NJ, USA: John Wiley & Sons, Inc., jan 1999.

[26] I. Marković, J. Ćesić, and I. Petrović, "Von Mises Mixture PHD Filter," *IEEE Signal Processing Letters*, vol. 22, no. 12, pp. 2229–2233, 2015.

[27] G. Kurz, I. Gilitschenski, and U. D. Hanebeck, "Unscented von Mises-Fisher filtering," *IEEE Signal Processing Letters*, vol. 23, no. 4, pp. 463–467, 2016.

[28] I. Gilitschenski, G. Kurz, S. J. Julier, and U. D. Hanebeck, "Unscented Orientation Estimation Based on the Bingham Distribution," *IEEE Transactions on Automatic Control*, vol. 61, no. 1, pp. 172–177, 2016.

[29] I. Marković, M. Bukal, J. Ćesić, and I. Petrović, "Multitarget tracking with the von Mises-Fisher filter and probabilistic data association," *Journal of Advances in Information Fusion*, pp. 1557–6418, 2016.

[30] N. Dalal and B. Triggs, "Histograms of Oriented Gradients for Human Detection," in *2005 IEEE Computer Society Conference on Computer Vision and Pattern Recognition (CVPR'05)*, vol. 1. IEEE, 2005, pp. 886–893.

[31] O. Tuzel, F. Porikli, and P. Meer, "Human Detection via Classification on Riemannian Manifolds," in *2007 IEEE Conference on Computer Vision and Pattern Recognition*. IEEE, jun 2007, pp. 1–8.

[32] A. Romero, M. Gouiffés, and L. Lacassagne, "Covariance Descriptor Multiple Object Tracking and Re-identification with Colorspace Evaluation," in *Lecture Notes in Computer Science*, 2013, vol. 7729 LNCS, no. PART 2, pp. 400–411.

[33] L. Chen, H. Ai, C. Shang, Z. Zhuang, and B. Bai, "Online multi-object tracking with convolutional neural networks," in *2017 IEEE International Conference on Image Processing (ICIP)*, vol. 2017-Septe. IEEE, sep 2017, pp. 645–649.

[34] Q. Chu, W. Ouyang, H. Li, X. Wang, B. Liu, and N. Yu, "Online Multi-object Tracking Using CNN-Based Single Object Tracker with Spatial-Temporal Attention Mechanism," in *2017 IEEE International Conference on Computer Vision (ICCV)*, vol. 2017-Octob. IEEE, oct 2017, pp. 4846–4855.

[35] Z. Lu, V. Rathod, R. Votel, and J. Huang, "RetinaTrack: Online single stage joint detection and tracking," 2020.

[36] S. Sun, N. Akhtar, H. Song, A. Mian, and M. Shah, "Deep Affinity Network for Multiple Object Tracking," vol. 43, no. 1, 2021.

[37] Y. Wu, B. Wu, J. Liu, and H. Lu, "Probabilistic tracking on riemannian manifolds," in *Proceedings - International Conference on Pattern Recognition*, 2008.

[38] H. Snoussi and A. Mohammad-Djafari, "Particle Filtering on Riemannian Manifolds," in *AIP Conference Proceedings*, vol. 872. AIP, 2006, pp. 219–226.

[39] V. Solo, "On nonlinear state estimation in a Riemannian manifold," in *Proceedings of the 48h IEEE Conference on Decision and Control (CDC) held jointly with 2009 28th Chinese Control Conference*, no. December. Shanghai, China: IEEE, dec 2009, pp. 8500–8505.

[40] S. Hauberg, F. Lauze, and K. S. Pedersen, "Unscented kalman filtering on riemannian manifolds," *Journal of Mathematical Imaging and Vision*, vol. 46, no. 1, pp. 103–120, 2013.

[41] S. Leonardos, X. Zhou, and K. Daniilidis, "Articulated motion estimation from a monocular image sequence using spherical tangent bundles," in *2016 IEEE International Conference on Robotics and Automation (ICRA)*, vol. 2016-June. IEEE, may 2016, pp. 587–593.

[42] H. M. T. Menegaz, J. Y. Ishihara, and H. T. M. Kussaba, "Unscented Kalman Filters for Riemannian State-Space Systems," *IEEE Transactions on Automatic Control*, vol. 64, no. 4, pp. 1487–1502, apr 2019.

[43] M. Brossard, A. Barrau, and S. Bonnabel, "A Code for Unscented Kalman Filtering on Manifolds (UKF-M)," in *Proceedings - IEEE International Conference on Robotics and Automation*, 2020.

[44] R. Zanetti and K. J. DeMars, "Joseph Formulation of Unscented and Quadrature Filters with Application to Consider States," *Journal of Guidance, Control, and Dynamics*, vol. 36, no. 6, pp. 1860–1864, nov 2013.

[45] J. Jost, *Riemannian Geometry and Geometric Analysis*, ser. Universitext. Berlin, Heidelberg: Springer Berlin Heidelberg, 2011.

[46] S. Janson, "Riemannian Geometry: Some Examples, Including Map Projections," Tech. Rep., 2015.

[47] Y. Bar-Shalom, F. Daum, and J. Huang, "The probabilistic data association filter," *IEEE Control Systems Magazine*, vol. 29, no. 6, pp. 82–100, 2009.

[48] D. Schuhmacher, B.-T. Vo, and B.-n. Vo, "A Consistent Metric for Performance Evaluation of Multi-Object Filters," *IEEE Transactions on Signal Processing*, vol. 56, no. 8, pp. 3447–3457, aug 2008.